

LARGE-SCALE SIMULATION OF OCEANIC GAS HYDRATE DISSOCIATION IN RESPONSE TO CLIMATE CHANGE

Matthew T. Reagan, George J. Moridis, and Keni Zhang

Lawrence Berkeley National Laboratory
1 Cyclotron Rd.
Berkeley, CA 94720 USA
e-mail: MTReagan@lbl.gov

ABSTRACT

Vast quantities of methane are trapped in oceanic hydrate deposits, and there is concern that a rise in the ocean temperature will induce dissociation of these hydrate accumulations, potentially releasing large amounts of carbon into the atmosphere. Because methane is a powerful greenhouse gas, such a release could have dramatic climatic consequences. The recent discovery of active methane gas venting along the landward limit of the gas hydrate stability zone (GHSZ) on the shallow continental slope west of Svalbard suggests that this process may already have begun, but the source of the methane has not been determined. This study performs a 2D simulation of hydrate dissociation in conditions representative of the Svalbard margin to assess whether such hydrates could be responsible for in the observed gas release. The results show that shallow, low-saturation hydrate deposits, if subjected to recent measured or predicted temperature changes at the seafloor, can release quantities of methane at the magnitudes recorded, and that the releases will be localized near the landward limit of the top of the GHSZ as observed. Both gradual and rapid warming is simulated, and localized gas release is observed for both cases. These suggest that hydrate dissociation and methane release as a result of climate change may be a real phenomenon, and that it already may be occurring.

INTRODUCTION

Gas hydrates are solid crystalline compounds in which gas molecules are lodged within a clathrate crystal lattice (Sloan, 1998). Natural gas hydrate deposits occur in geologic settings where the necessary low temperatures and high pressures exist for their formation and stability. Vast quantities of methane are trapped in oceanic hydrate deposits (Klauda and Sandler, 2005). Because methane is a powerful greenhouse gas (about 26 times more effective than CO₂), there is considerable concern that a rise in the ocean temperature will induce dissociation of these hydrate accumulations, potentially releasing large amounts of carbon into the atmosphere.

Initial investigations estimated the total amount of methane hydrate currently residing in the deep ocean and along continental margins, beginning with an early “consensus value” of 10,000 gigatons (Gt, 20×10^{15} m³ STP) of methane carbon (Gornitz and Fung, 1994; Kvenvolden, 1999; Borowski, 2004). However, more recent studies have produced widely different results—one yielding an upper estimate of 27,300 Gt of methane in hydrate along continental margins (74,400 Gt globally) (Klauda and Sandler, 2005) and the other a lower estimate of 3,000 Gt of methane in hydrate and 2,000 Gt of underlying gaseous methane (Buffett and Archer, 2004).

In oceanic deposits, the depth at which hydrates remain stable depends on the pressure (as imposed by the water depth) and the temperature. An increase in water temperature at the seafloor changes the extent of the gas hydrate stability zone (GHSZ), and such a shift could induce hydrate dissociation and lead to methane release. Deep ocean surveys have found pockmarks and other structures that indicate large fluid releases at the seafloor in the past (Hovland et al., 2005), and computational studies show the potential for hydrate instability under warming conditions (Reagan and Moridis, 2008).

Such a release could have dramatic climatic consequences because it could amplify atmospheric and oceanic warming and possibly accelerate dissociation of the remaining hydrates. This positive-feedback mechanism has been proposed as a significant contributor to rapid and significant climate changes in the late Quaternary period (Kennett et al., 2000). The Clathrate Gun Hypothesis (Kennett et al., 2002) proposes that past increases in water temperatures near the seafloor may have induced such a large-scale dissociation, with the methane spike and isotopic anomalies reflected in polar ice cores and in benthic foraminifera. While this hypothesis is controversial, and the relationship between hydrates and climate has not yet been established, the role of methane in climate cycles is currently an active area of research, and hydrates are considered to be a potential source (Mascarelli, 2009).

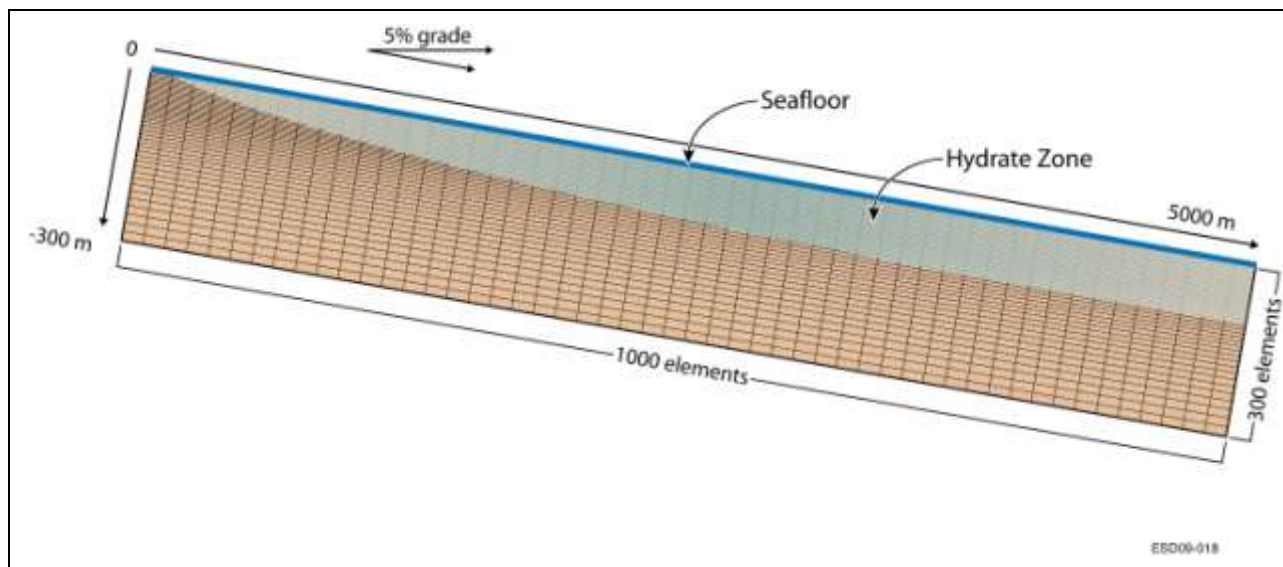


Figure 1. Illustration of the domain discretization, GHSZ extent, and boundaries for the 2D sloping system (not to scale). Gridlines are a schematic representation only.

The recent discovery of active gas venting along the shallow continental slope west of Svalbard creates new cause for concern (Westbrook et al., 2009). The observed plumes release a sizeable quantity of methane—enough that some methane reaches the ocean surface. While methane seeps are known to exist in other locations, this system is notable in that the locations of the plumes coincide with the landward limit of the GHSZ, suggesting that recent changes in ocean temperature at the seafloor have interacted with shallow hydrates in the subsurface. Two hydrate-related phenomena are proposed: (1) that dissociating shallow hydrates are responsible for the methane itself; and (2) that methane arriving from deeper sources forms hydrate in the shallow GHSZ, and this hydrate (due to the change in effective permeability) may act to block or channel methane that migrates upward from deeper sources. To test this hypothesis, this study performs a large-scale, 2D simulation of shallow hydrates in conditions representative of the western Svalbard margin to assess the potential for hydrate dissociation, methane release, and methane plume formation in arctic continental shelf environments subjected to ocean warming.

MODELS AND METHODS

We evaluate the stability and dissociation of shallow oceanic hydrates subjected to short-term temperature variations and the flow of methane in the subsurface using the massively parallel version of the TOUGH+HYDRATE code (pT+H) (Moridis et al., 2008). T+H models the nonisothermal hydration reaction, phase behavior and flow of fluids and heat in complex geologic media (Moridis and Kowalsky, 2007; Moridis and Sloan, 2007) and has been used in

earlier 1D studies of hydrate dissociation in response to ocean temperature change (Reagan and Moridis, 2008). This study is the first simulation of fully coupled hydrate dissociation, heat transport, and multiphase flow applied to a climate-driven system of this magnitude.

Domain Discretization and Initial Configuration

The model is a 2D sloping system 5,000 m in length and extending to 300 m below the seafloor. The western Svalbard continental shelf has a 3%–5% slope, as indicated by local averages from GEBCO bathymetry data for the western Svalbard region (GEBCO, 1997) and as reported by Westbrook (2009) in the region of methane plume formation. We select a 5% grade (20 m per 1 m depth) to constrain the horizontal extent of the system. The top of the slope is located at a depth of 300 m, above the top of the GHSZ at local temperatures, with the bottom of the slope at 550 m for a 5% grade. Figure 1 shows a schematic of the mesh (not to scale), including the system boundaries and the extent of the GHSZ. To represent the system at a suitable level of detail, we use 300,000 gridblocks (1000×300), with a horizontal discretization of $dx = 5$ m, a 2D slice thickness of $dy = 1$ m, and a variable vertical discretization, beginning with $dz=0.25$ m from the seafloor to $z=-50$ m, $dz = 0.5$ m between $z = -50$ m and $z = -75$ m, and a logarithmic progression ($dz=0.5-15.8$ m) from $z=-75$ to $z = -300$ m.

The initial condition involves a hydrostatic pressure distribution based on depth and 3.5 wt% salinity, initial temperature based on a geothermal gradient of $8.7^{\circ}\text{C}/100$ m (Haacke et al., 2008), and a uniform initial hydrate saturation of 3% in the sediment column within the GHSZ. The extent of the GHSZ is

computed directly from the depth and initial temperature using T+H (Moridis, 2003; Moridis et al., 2008) and the initial state of the system was brought to thermal equilibrium and hydrostatic conditions. A preexisting region of free gas, often inferred to exist underneath shallow stratigraphic hydrate deposits, is not included in this simulation, as the actual quantity of gas under systems of this type has not been directly measured and our goal is to assess the quantity of gas that may be released due to hydrate dissociation alone.

System Properties

The intrinsic permeability for this base case, $k = 1$ mD, is within the reported range of hydrate-bearing oceanic sediments (Ginsberg and Soloviev, 1998) and represents a baseline stratigraphic or “Class 4” hydrate deposit (Moridis and Sloan, 2007), in contrast to the less common, more permeable, and often more saturated structures near sites of active methane seepage and/or venting. The porosity $\phi = 0.55$ reflects measurements taken at deeper locations further offshore (Haake et al., 2008). The physical properties parameters used in the simulations are summarized in Table 1.

The top of the sediments is bounded by an open boundary representing heat and mass transfer between the sediments and the bulk ocean. The pressure at the upper boundary (set according to hydrostatic conditions at the initial salinity) is held constant, representing constant ocean levels. The domain bottom is a closed boundary at $z = -300$ m, beyond the expected range of temperature propagation on short time scales, and is held at a constant temperature selected to match the known initial geothermal gradient and supply the expected geological heat flux from lower strata.

Climate Change Scenarios

Recent climate simulations coupling ocean circulation, atmospheric circulation, and atmospheric chemistry (Meehl et al., 2007) indicate that, under current climate conditions and a 1%/yr increase in atmospheric CO₂, the temperature at the seafloor would rise by 1°C over the next 100 yr, and possibly by another 3°C in the following century. Historical temperature data from the Svalbard region (Westbrook et al., 2009) suggest that a 1°C change in bottom-water temperature has already occurred over the last 30 years. Previous work on the response of shallow hydrates to ocean temperature change (Reagan and Moridis, 2008) indicates that temperature changes as small as 1–3°C can have significant effects on shallow hydrates.

Table 1. Physical properties and simulation parameters for the 2D hydrate-bearing system

Parameter	Value
Initial pore water salt mass fraction, X_0	0.035
Permeability, k	10^{-15} (= 1 mD)
Porosity, ϕ (Haake et al., 2008)	0.55
Dry thermal conductivity, k_{sd}	1.0 W/m/K
Wet thermal conductivity, k_{sw}	3.3 W/m/K
Composite thermal conductivity k_{\odot} model (Moridis et al., 2005)	$k_{\odot} = (\sqrt{S_H} + \sqrt{S_A}) * (k_{sw} - k_{sd}) + k_{sd}$
Capillary pressure model (van Genuchten, 1980)	$P_{cap} = -P_0 \left[(S^*)^{-1/\lambda} - 1 \right]^2$ $S^* = \frac{(S_A - S_{irA})}{(S_{mxA} - S_{irA})}$
P_0	2000 Pa
Relative permeability model (Stone, 1970)	$k_{rA} = (S_A^*)^n$ $k_{rG} = (S_G^*)^n$ $S_A^* = (S_A - S_{irA}) / (1 - S_{irA})$ $S_G^* = (S_G - S_{irG}) / (1 - S_{irA})$
λ	0.45
n	4
S_{irG}	0.02
S_{irA}	0.20

Therefore, we vary the temperature at the upper boundary to represent these changes in the bulk ocean temperature above the seafloor. As a base case, we assume an initial seafloor temperature of $T_0 = 0^\circ\text{C}$ (Westbrook et al., 2009). We increase the overlying ocean temperature by 1°C/100 yr, a conservative representation of possible temperature changes over the last century, and also a conservative projection of potential warming in the near future. We simulate the evolution of the system for a total of 300 yr to capture a range of conditions and create a significant variation in the extent of the GHSZ. In addition, to assess the effect of more rapid change, we also extrapolate the reported 1°C/30 yr trend (Westbrook et al., 2009) to 3°C/100 yr for comparison. In both cases, the total simulation time is restricted, as extrapolation of recent temperature trends over many centuries is speculative at best, and we are most interesting in capturing century-scale phenomena that

may already be occurring, and that may already be observable.

RESULTS AND DISCUSSION

While simulating the evolution of the representative hydrate deposit, we record localized methane fluxes through the upper boundary, hydrate dissociation rates, and phase saturations throughout the 2D system. To simulate such a large system, 80–100 processors were required to produce significant results in a manageable amount of time, as the solution of the problem requires the coupled solution of 1.2×10^6 equations at each timestep.

Base Case: Gradual Change

The base case represents a 3°C temperature change at the seafloor (at all depths from 300 to 550 m) over a 300 yr period. The temperature was varied linearly at a rate of $1^\circ\text{C} / 100$ yr, with an initial temperature of $T_0 = 0^\circ\text{C}$ at $t = 0$. The upslope limit of the GHSZ at initial conditions is located at $x = 290$ m, or a water depth of approximately 314 m.

Figure 2 describes the evolution of hydrate saturation, S_H , with time. Minimal change is observed at $t = 50$ yr, but by $t = 100$ yr significant recession is apparent (corresponding to the new upper extent of the GHSZ at time t). At the end of the 300 yr simulation period, the upper (leftmost) extent of methane gas hydrate has receded over 1,700 m downslope.

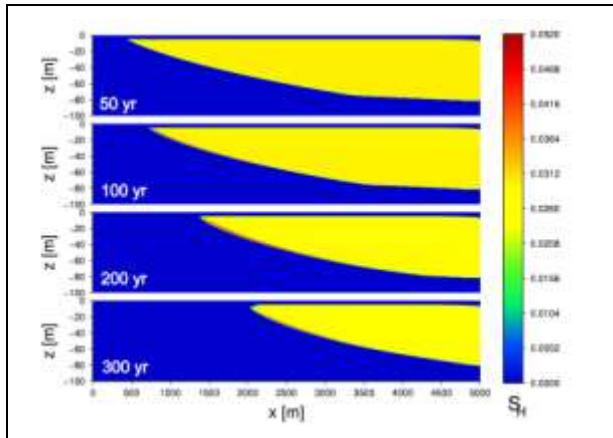


Figure 2. Hydrate saturation, S_H , for the 2D system at $t = 50, 100, 200,$ and 300 yr for the base case. The top of the 5% slope is at $x = 0$.

Figure 3 shows the evolution of gas saturation, S_G , with time. At $t = 50$ yr (18,200 days), only a thin layer of gas is seen along the bottom of the region of hydrate-bearing sediments. By $t = 100$ yr (36,400 days), a significant region of gas has formed in place of the receding hydrate, with the highest

concentration along the bottom of the remaining hydrate and the landward (leftmost) limit of the GHSZ at $x = 750$ m downslope. This gas, now at saturations in excess of the irreducible gas saturation (2%), is moving upward toward the seafloor ($z = 0$). By $t \sim 200$ yr (75,129 days), a “plume” of high gas saturation is observed, as gas moves along the bottom of the remaining hydrate deposit and reaches the seafloor at $x \sim 1400$ m downslope. At $t = 300$ yr (109,201 days), the plume of highest gas saturation is located 2,000 m downslope, and the entire region of the seafloor from $x = 500$ m to $x = 2000$ m is receiving mobile methane gas from below.

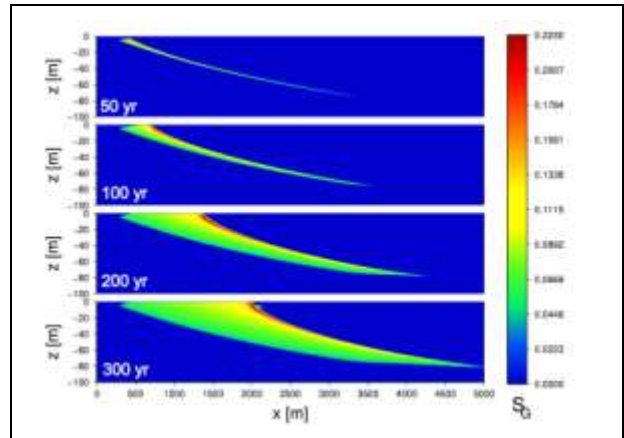


Figure 3. Gas saturation, S_G , for the 2D system at $t = 50, 100, 200,$ and 300 yr for the base case. The top of the 5% slope is at $x = 0$.

Note the increase in hydrate saturation ($S_H > S_{H,0}$) in a thin zone along the bottom of the hydrate-bearing sediments for $t > 100$ yr seen in Figure 2. As gaseous methane (Figure 3) travels along the bottom of the remaining hydrate mass (guided by the reduced effective permeability of the overlying hydrate-bearing sediments), secondary hydrate re-forms as some gas enters the (now less extensive) GHSZ. The localized increase in S_H further reduces the effective permeability at the base of the hydrate zone, and the result is a channeling of gas into a plume of high saturation.

Simulation outputs indicate that the first appearance of gaseous methane at the seafloor occurs around $t = 97$ yr. In Figure 4, the evolution of gas flux, Q_{CH_4} , presented here as mol CH_4 per m^2 at downslope position x for a 1 m-wide 2D slice of the overall system, is plotted as a function of time, t . The peak of the Q_{CH_4} profile corresponds almost exactly to the location of contact between the gas-phase “plume” observed in Figure 3 and the seafloor. The peak Q_{CH_4} , as does the plume, moves downslope over time. Localized methane gas flux peaks at 45 mol/yr-m^2 (at $t \sim 250$ yr), but significant fluxes of gaseous methane

occur over a wide area, locally decreasing with time as the subsurface plume moves downslope.

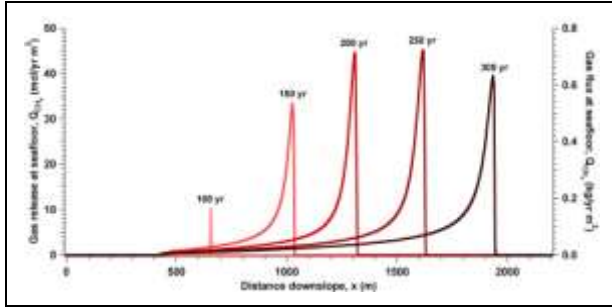


Figure 4. Flux of gaseous methane, Q_{CH_4} , at the seafloor at $t = 100, 150, 200, 250,$ and 300 yr. Q_{CH_4} is presented here as mol CH_4 per m^2 at downslope position x for a 1 m-wide 2D slice of the real system, for the base case.

The evolution of the total methane release at the seafloor, in both aqueous and gaseous form, for the entire $5000\text{ m} \times 1\text{ m}$ seafloor boundary is shown in Figure 5. Methane release into the ocean begins just before $t = 100$ yr, increases continuously over the simulated timeframe, and is still increasing at the end of the simulation at $t = 300$ yr, having reached 8900 mol/yr.

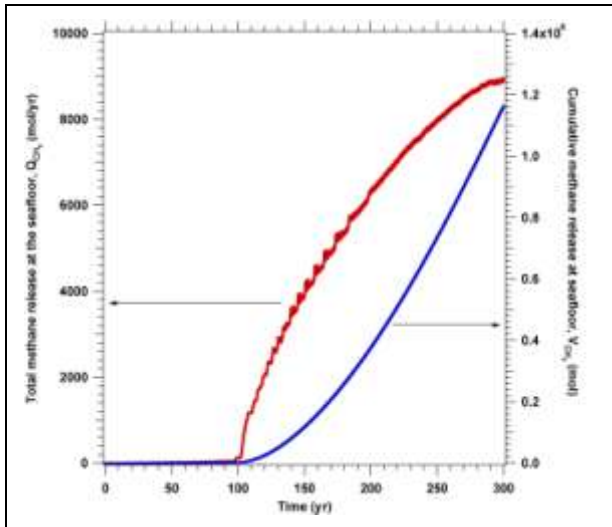


Figure 5. Total methane release (aqueous and gaseous phases), $Q_{CH_4,T}$, and cumulative methane release, V_{CH_4} , for the entire simulated seafloor boundary, a 1 m wide, 5000 m long section, for the base case

Figure 5 also describes the time evolution of the cumulative methane release, V_{CH_4} , for the entire $5000\text{ m} \times 1\text{ m}$ seafloor boundary. By $t = 300$ yr, over 1.16×10^6 mol of CH_4 has been released in the overlying ocean.

Case II: Rapid Change

While the base case assumed conservative projections, some observations suggest that warming may in fact be occurring at a considerably faster pace. A change in the temperature of the West Spitsbergen current of 1°C over the past 30 yr has been reported (Westbrook, 2009) with an average rate of $0.03^\circ\text{C}/\text{yr}$. We model this rapid change with a linear 3°C temperature increase at the seafloor (at all depths from 300 to 550 m) over a 100 yr period with an initial temperature of $T_0 = 0^\circ\text{C}$ at $t = 0$. After 100 years of simulation, the ocean temperature is held constant for additional 100 yr to assess the consequences of the rapid warming. No additional warming is simulated for the reasons stated previously. The simulation is otherwise performed in an identical manner to the base case.

Figure 6 describes the evolution of hydrate saturation, S_H , with time for the case of rapid change. Over the 200 yr simulation period, the upper (leftmost) extent of methane gas hydrate recedes by approximately 1500 m downslope. More so than the base case, here we clearly see the effects of the lowering of the top of the GHSZ, as an upper dissociation front is apparent at $t = 50$ yr, 100 yr, and 130 yr. Note that in all contour plots, the 2D system has a 5% slope, with the top of the slope located at $x = 0$, and as such the angle to the observed dissociation front reflects this slope.

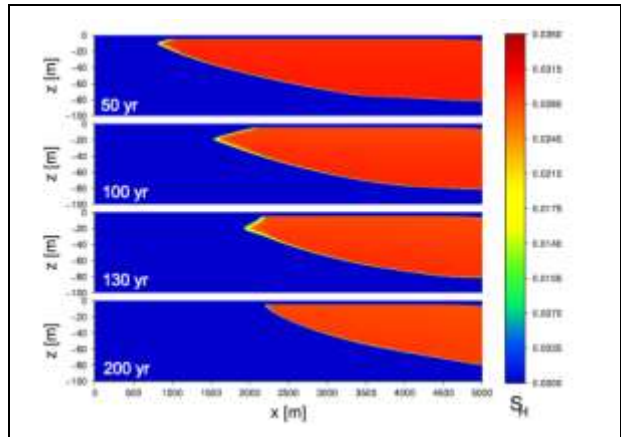


Figure 6. Hydrate saturation, S_H , for the 2D system at $t = 50, 100, 130,$ and 200 yr for Case II. The top of the 5% slope is at $x = 0$.

Simulations of 1D hydrate-bearing sediment columns under shallow Arctic conditions (Reagan and Moridis, 2008) have demonstrated that the rate of dissociation is regulated by heat transfer limitations, as hydrate dissociation is strongly endothermic, and thus we see the formation of a sharp dissociation front in both the previous 1D study and in this 2D simulation. Secondary hydrate formation is less

apparent in this case, with only a slight increase in S_G to 0.035 along the bottom of the hydrate-bearing zone at $t = 200$ yr (72,746 days).

Figure 7 shows the evolution of gas saturation, S_G , with time. At $t = 50$ yr (18,200 days), a large region of free gas already fills the sediments as the top and bottom of the GHSZ has receded substantially and mobile gas is moving upward toward the seafloor. As in the base case, the gas forms a localized plume of high S_G , which in this case remains well-defined as the gas travels through the region between the upper dissociation boundary and the seafloor. This plume contacts the seafloor at $x \sim 750\text{--}1500$ m, and as in the base case, moves downslope over time, but in this case gas saturations decrease noticeably by $t = 130$ yr. By $t = 200$ yr, the entire region of the seafloor from $x = 500$ m to $x = 2200$ m is receiving mobile methane gas from below, but S_G within the plume has declined substantially, and the plume is no longer well-defined.

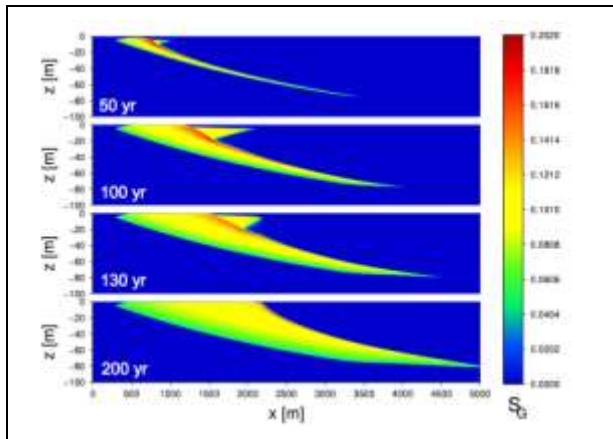


Figure 7. Gas saturation, S_G , for the 2D system at $t = 50, 100, 130,$ and 200 yr for Case II. The top of the 5% slope is at $x = 0$.

Simulation outputs indicate that the first appearance of gaseous methane at the seafloor occurs around $t \sim 80$ yr, and that the onset of gas release is rapid. In Figure 8, the evolution of gas flux, Q_{CH_4} ($\text{mol}/\text{yr}\cdot\text{m}^2$), is presented as a function of time, t , and downslope position, x . As in the base case, the peak of the gaseous flux corresponds closely to the location of the gas-phase plume observed in the 2D plots of S_G . However, in Case II, methane gas flux peaks immediately at $15 \text{ mol}/\text{yr}\cdot\text{m}^2$ and then slowly decreases with time.

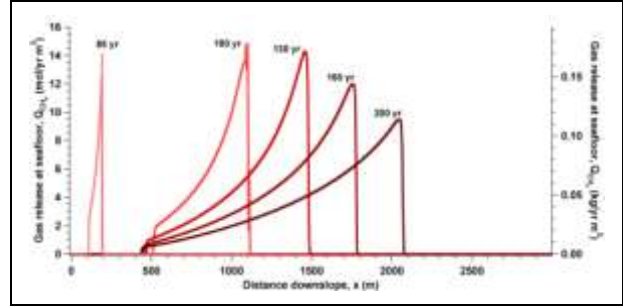


Figure 8. Flux of gaseous methane, Q_{CH_4} , at the seafloor at $t = 85, 100, 130, 160,$ and 200 yr for Case II. Q_{CH_4} is presented here as $\text{mol } CH_4 \text{ per } m^2$ at downslope position x for a 1 m wide 2D slice of the real system.

However, in contrast to the base case, the distribution of venting is broader, reflecting the greater extent of high-saturation gas present within the sediment at a given time t compared to the base case. As seen in Figures 3 and 7, the region of free gas extends 750 m further downslope at $t = 200$ yr when compared to the base case, reflecting more rapid dissociation of the hydrate and also indicating that the transport of gas to the seafloor is not necessarily increased simply due to the rapidity of dissociation.

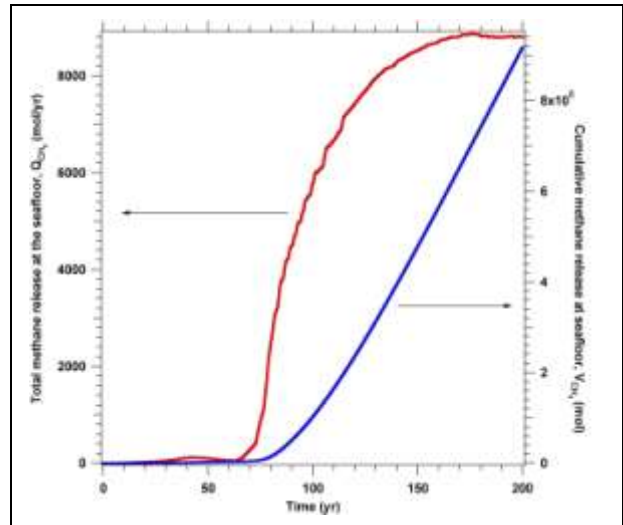


Figure 9. Total methane release (aqueous and gaseous phases), $Q_{CH_4,T}$, and cumulative methane release, V_{CH_4} , for Case II over the entire simulated seafloor boundary, a 1 m wide, 5000 m long section.

The evolution of the total methane flux, in both aqueous and gaseous form, for the entire $5000 \text{ m} \times 1 \text{ m}$ seafloor boundary is shown in Figure 9. Methane release into the ocean begins at approximately $t = 30$ yr in the aqueous phase, but increases rapidly after $t = 65$ yr until a peak at $t = 175$ yr at

8800 mol/yr for the 1 m wide 2D slice of the overall system. Despite a much more rapid disappearance of hydrate compared to the base case, the peak flux is nearly identical. Figure 9 also shows the evolution of cumulative release over time, with this case releasing a total of 9.2×10^5 mol of CH_4 by $t = 200$ yr. In comparison, at $t = 200$ yr the base case has released only 3.8×10^5 mol of CH_4 . While instantaneous fluxes may be similar for different warming scenarios, more rapid warming clearly results in faster rates of gas release at the seafloor, as would be expected.

CONCLUSIONS

Comparison to 1D results

Previous simulations of 1D hydrate-bearing sediment columns (Reagan and Moridis, 2008) indicated that hydrate dissociation due to both gradual and rapid change does not produce violent eruptions of methane gas, rather, dissociation and the resultant gas release tend to occur in an orderly fashion, regulated by heat transfer limitations and gas migration through sediments containing multiple phases. Extending the model system to a 2D sloping domain introduces horizontal migration of fluids and dissociation of hydrate along multiple fronts. However, the rate of dissociation and the rate of gas release into the environment are still constrained by heat and fluid flow limitations, and as such these deposits release gas at the seafloor in an orderly fashion. In both the base case and Case II in particular, we see the formation of a sharp upper dissociation boundary and instantaneous total methane fluxes that asymptotically approach a constant value, similar to the example of a 1D Arctic hydrate system at $T = 0.4^\circ\text{C}$ and 320 m depth (Reagan and Moridis, 2008). Substantial but not catastrophic releases appear to be the likely consequence of climate-driven hydrate dissociation.

Comparison to Observations

A team led by Westbrook (Westbrook et al., 2009) recently observed over 250 plumes of methane gas erupting from the seabed off the West Spitsbergen (Svalbard) continental margin at the present landward limit of the GHSZ. These gas plumes, which extend along 30 km of the slope, have been hypothesized to be partly the result of hydrate dissociation as a consequence of recent ocean warming in the area, and partly due to diversion and channeling of upwelling methane by hydrate-bearing sediments. Using hydrate saturations taken (about 4.5% average) from further downslope, the observers estimated a potential release of 900 kg/yr CH_4 per 1 m of margin length.

The simulations presented in this paper closely represent the type and extent of hydrate-bearing

system thought to exist along the Svalbard margin, and allow us to make several conclusions about the nature of this system:

(1) Our simulations, using a slightly lower average $S_{H,0}$, suggest that at least 141 kg/yr CH_4 per 1 m width of slope can be released solely due to dissociating hydrate. Integrated over the 30 km plume region, this would be 0.004 Tg/yr of CH_4 from this one hydrate system alone, small in comparison to the global atmospheric flux of methane but significant to the ocean biochemistry of the region.

(2) A second conclusion from this study is that hydrate alone can provide a significant quantity of methane gas in climate change-driven release scenarios, in addition to any geological methane source that may be providing free gas or dissolved aqueous methane to the region below the GHSZ.

(3) A third conclusion is that the hydrate-bearing sediments can divert and channel the flow of aqueous and gaseous methane, despite the very low hydrate saturations expected for disperse, unconfined stratigraphic deposits. In both the base and rapid-warming cases, we observe channeling of mobile gas along the bottom of the GHSZ due to the reduced effective permeability of hydrate-bearing sediments, the trapping of methane through the formation of secondary hydrate when methane enters the GHSZ, and the formation of localized subsurface plumes of higher methane saturation that directly correlate to localized gaseous fluxes at the seafloor. These processes provide a clear model for the formation of gas plumes at the landward limit of the GHSZ, as observed.

ACKNOWLEDGMENT

This research was funded by the Assistant Secretary for Fossil Energy, Office of Natural Gas and Petroleum Technology, through the National Energy Technology Laboratory. The authors would like to thank Katie L. Boyle for the development of the 2D data visualization tools.

REFERENCES

- Borowski, W.S., A review of methane and gas hydrates in the dynamic, stratified system of the Blake Ridge region, offshore southeastern North America. *Chem. Geology*, 205, 311-346, 2004.
- Buffett, B., and D. Archer, Global inventory of methane clathrate: Sensitivity to changes in environmental conditions, *Earth Planetary Sci. Lett.*, 227, 185-199, 2004.
- GEBCO, Published by the British Oceanographic Data Centre on behalf of Intergovernmental Oceanographic Commission and International Hydrographic Organization, 1997.

- Ginsburg, G.D. and V.A. Soloviev, Submarine Gas Hydrates. St. Petersburg, 1998.
- Gornitz V., and I. Fung, Potential distribution of methane hydrate in the world's oceans, *Global Biogeochem. Cycles*, 8, 335-347, 1994.
- Haake, R.R., Westbrook, G.K., and M.S. Riley, Controls on the formation and stability of gas hydrate-related bottom-simulating reflectors (BSRs): A case study from the west Svalbard continental slope, *J. Geophys. Res.*, 113, B05104, doi: 10.1029/2007JB005200, 2008.
- Hovland, M., Svensen, H., Forsberg, C.F., Johansen, H., Fichler, C., Fossa, J.H., Jonsson, R., and H. Rueslatten, Complex pockmarks with carbonate-ridges off mid-Norway: Products of sediment degassing, *Marine Geology*, 218, 191-206, 2005.
- Kennett, J.P., Cannariato, K.G., Hendy, L.L., and R.J. Behl, Carbon isotopic evidence for methane hydrate instability during quaternary interstadials. *Science*, 288, 128-133, 2000.
- Kennett, J.P., Cannariato, K.G., Hendy, L.L., and R.J. Behl, *Methane hydrates in quaternary climate change: The Clathrate Gun Hypothesis*, AGU Publishing, Washington, DC, 2002.
- Klauda, J.B., and S.I. Sandler, Global distribution of methane hydrate in ocean sediment. *Energy and Fuels*, 19, 459-470, 2005.
- Kvenvolden, K.A., Potential effects of gas hydrate on human welfare, *Proc. Nat. Acad. Sci.*, 96, 3420-3426, 1999.
- Mascarelli, A.L., A Sleeping Giant? *Nature Reports Climate Change*, 3(4), doi: 10.1038/climate.2009.24, 2009.
- Meehl, G., et al., Global climate projections, *Climate Change 2007: The Physical Basis*, 789-844, Cambridge Univ. Press, Cambridge, UK, 2007.
- Moridis, G.J., Numerical Studies of Gas Production from Methane Hydrates, *SPE Journal*, 32(8), 2003.
- Moridis, G.J., Seol, Y., and T. Kneafsey, Studies of reaction kinetics of methane hydrate dissociation in porous media (Paper 1004), *Proceedings of the 5th International Conference on Gas Hydrates*, Trondheim, Norway, 12-16 June 2005.
- Moridis, G.J., and M.B. Kowalsky, Response of Oceanic Hydrate-Bearing Sediments to Thermal Stresses, *SPE Journal*, 12(2), 253-268, doi:10.2118/111572-PA, 2007.
- Moridis, G.J., and E.D. Sloan, Gas production potential of disperse low-saturation hydrate accumulations in oceanic sediments, *Energy Conv. Manag.*, 48, 1834-1849, doi:10.1016/j.enconman.2007.01.023, 2007.
- Moridis, G.J., Kowalsky, M.B., and K. Pruess, *TOUGH+HYDRATE v1.0 User's Manual: A Code for the Simulation of System Behavior in Hydrate-Bearing Geologic Media*, Report LBNL-0149E, Lawrence Berkeley National Laboratory, Berkeley, CA.
- Reagan, M. T., and G. J. Moridis, Dynamic response of oceanic hydrate deposits to ocean temperature change, *J. Geophys. Res.*, 113, C12023, doi:10.1029/2008JC004938, 2008.
- Sloan, E.D. and C. Koh, *Clathrate Hydrates of Natural Gases*, CRC Press, New York, NY, 2008.
- Stone, H.L., Probability model for estimating three-phase relative permeability, *Trans. SPE AIME*, 249, 214-218, 1970.
- Westbrook, G.K., Thatcher, K.E., Rohling, E.J., Piotrowski, A.M., Palike, H., Osborne, A.H., Nisbet, E.G., Minshull, T.A., Lanoiselle, M., James, R.H., Huhnerbach, V., Green, D., Fisher, R.E., Crocker, A.J., Chabert, A., Bolton, C., Beszczynska-Moller, A., Berndt, C., and A. Aquilina, Escape of methane gas from the seabed along the West Spitsbergen continental margin *Geophys. Res. Lett.*, in press, doi: 10.1029/2009GL039191, 2009.
- Van Genuchten, M.T., A closed-form equation for predicting the hydraulic conductivity of unsaturated soils, *Soil Sci. Soc.*, 44, 892-898, 1980.